# A Random Forest Based Classification Approach to Prostate Segmentation in MRI

Soumya Ghose[1,2], Jhimli Mitra[1,2], Arnau Oliver[2], Robert Martí[2], Xavier Lladó[2], Jordi Freixenet[2], Joan C. Vilanova[3], Désiré Sidibé[1] and Fabrice Meriaudeau[1]

[1] Laboratoire Le2I - UMR CNRS 6306, Université de Bourgogne, 12 Rue de la Fonderie, 71200 Le Creusot, France
[2] Computer Vision and Robotics Group, University of Girona, Campus Montilivi, Edifici P-IV, Av. Lluís Santaló , s/n, 17071 Girona, Spain
[3] Girona Magnetic Resonance Imaging Center, Girona, Spain

**Abstract.** Accurate prostate segmentation in magnetic resonance (MR) images aids in volume estimation, surgical planing and multi-modal image registration. However, automatic or semi-automatic prostate segmentation in MR images is a challenging task due to inter-patient prostate shape and size variabilities. We propose a supervised learning framework of decision forest to achieve a probabilistic representation of the prostate voxels. Finally, propagation of region based levelsets in the stochastic space provides the segmentation of the prostate. Quantitative and qualitative results show a good approximation of the prostate volumes.

**Keywords:** Prostate segmentation, random forest, MRI.

## 1 Introduction

Prostate cancer is the most commonly diagnosed cancer in North America and accounted for 33,000 estimated deaths in 2011 [1]. 3D prostate segmentation in MR images aids in volume estimation of the prostate and in surgical planing. Manual segmentation of the prostate in MR images is time consuming and suffers from inter- and intra-observer differences. However, automatic or semi-automatic computer aided segmentation of the prostate is a challenging task owing to inter-patient large scale shape, size and deformation variabilities of the prostate gland, intensity heterogeneities inside the prostate region and imaging artifacts.

In the last decade, atlas-based prostate segmentation in MR images has become popular [2–4]. Such methods have provided promising results when validated with large number of datasets. Further, shape prior deformable models are also often used for prostate segmentation [5, 6]. More recently Li et al. [7] used a machine learning approach to achieve a probabilistic segmentation of the prostate that was further refined with a levelset to achieve binary segmentation of the prostate. In recent years, supervised machine learning methods with decision forest have been adopted for solving classification problems in medical images [8]. Often context and appearance based features are used to build

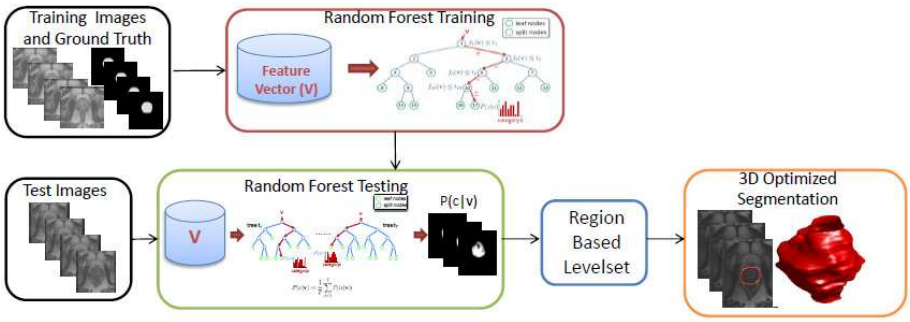


**Fig. 1.** Schematic representation of our approach.

a discriminative random decision forest to provide a voxel-wise probabilistic classification of a volume. Motivated by these approaches we propose a novel prostate segmentation method in which appearance, and spatial context based information from the training images are used to classify a new test image to achieve voxel-wise probabilistic classification. In our method, we adopt a similar approach in which appearance and spatial context based information are utilized to obtain a probabilistic segmentation of the prostate. Finally, a region based levelset propagating in probabilistic space produces binary segmentation of the prostate similar to the appraoch of Li et al. [7]. However Li et al. [7] had to perform rigid registration on the pelvic bones in computed tomography (CT) images and normalize the intensities before extracting features. Considering in prostate MRI pelvic bones are not visible and there is no reliable structure on which the rigid registration could be performed this method is difficult to adapt. Hence unlike [7] we have not registered the images to a common frame and normalized the intensities before extracting our features. Rather we have depended on the random forest classification model to handle variabilities in pose and appearance of the prostate.

## 2 Proposed segmentation framework

The proposed method is developed on two major components: the decision forest based probabilistic classification of the prostate, and propagation of region based levelsets to achieve a binary segmentation of the prostate. The schema of our proposed method is illustrated in Fig. 1. Our probabilistic classification problem may be formalized as a soft classification of voxel samples into either background or prostate. This classification problem is addressed by supervised random decision forest. Decision trees are discriminative classifiers which are known to suffer from over-fitting. However, a random decision forest achieves better generalization by growing an ensemble of many independent decision trees on a random subset of the training data and by randomizing the features made available at each node during training [8].

During **training**, the number of slices in a volume containing prostate is divided into three equal parts as apex, central and base regions. For example after selection of the first and the last slice if there are 9 slices, 3 top slices is grouped in apex, 3 slices after the apex slices are grouped in the central and the last 3 slices are grouped with the base slices. If there are 10 slices top 3 slices will go in the apex and the bottom 3 slices will be grouped with the bottom slices and 4 central slices will be grouped with the central slices. The images are resized to a resolution of 256×256 pixels. In presence of magnetic bias contrast-limited adaptive histogram equalization (CLAHE) [9] is performed to minimize the effect of bias. The CLAHE unlike the general histogram equalization methods divide the image into small region or tiles and enhances the contrast of each of the tiles. Furthermore contrast of each tile matches a normal distribution and neighboring tiles are combined using bilinear interpolation to reduce boundary effect. The method has an advantage over the general histogram equalization as contrast in large homogeneous regions are unaffected from magnetic bias found in a small region of the image.

The data consists of a collection of $3 \times 3$ neighborhood of pixels, centered at $V = (X, F)$. Where, $X = (x, y)$ denotes the position of the voxel associated with a feature vector $F$. The mean and standard deviation of the $3 \times 3$ voxel neighborhood are used as the feature vector $F$. Each tree $t_i$ in decision forest receives the full set $V$, along with the label and the root node and selects a test to split $V$ into two subsets to maximize information gain. A test consists of a feature (like the mean) and a feature response threshold. The left and the right child nodes receive their respective subsets of $V$ and the process is repeated at each child node to grow the next level of the tree. Growth is terminated when either information gain is minimum or the tree has grown to maximum depth. Each decision tree in the forest is unique as each tree node selects a random subset of features and threshold. Three different decision forests are built corresponding to the three different regions of the prostate the apex, the central region and the base. We have used only 50% of the available training data for each of the regions to minimize the problem of overfitting as the quantitative results were produced with the training data. However the entire 50 training dataset could be used to build random forest for evaluating the 23 test datasets.

During **testing**, after selection of the first and the last slice, the prostate in the test dataset is divided into three parts corresponding to the apex, the central region and the base. In presence of magnetic bias CLAHE is performed to minimize the effect of bias. All images are resized to a resolution of 256×256 before classification. Decision forests trained for each of the regions are applied to achieve a probabilistic classification of the apex, the central and the base slices. The pixels are routed to one leaf in each tree by applying the test (selected during training). Each voxel of the test dataset is propagated through all the trees by successive application of the relevant binary test. When reaching a leaf node $l_t$ in all tree where $t \in [1..., T]$, posterior probabilities ($p_{l_t}$) are gathered in order to compute the final posterior probability of the voxel defined by $P_{rf} = \frac{1}{T} \sum_{t=1}^{T} p_{l_t}$. Computation of class posterior probabilities in decision forest is illustrated in

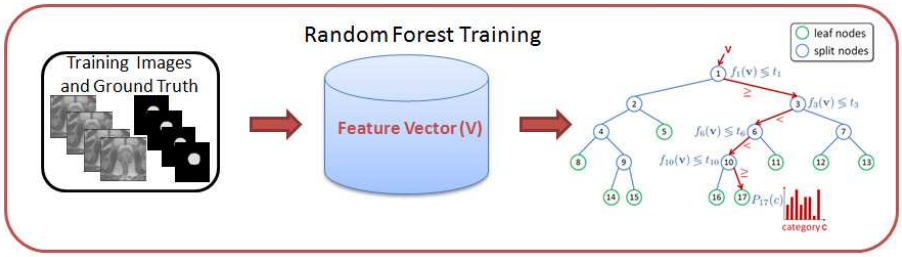


(a)

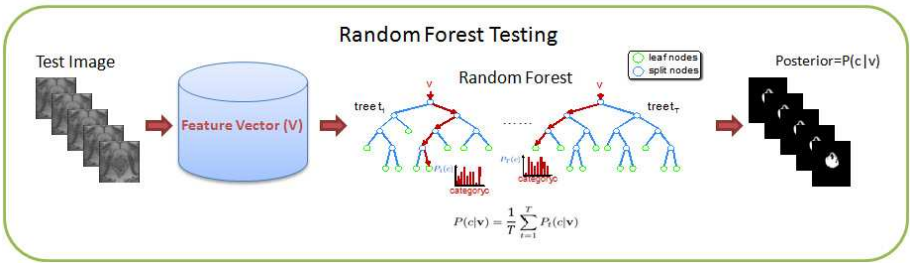


(b)

**Fig. 2.** Random forest classification framework (a) Random forest training (b) Random forest classification with test images.

Fig. 2. Intensity of the image is substituted with posterior probabilities obtained with random forest. According to Chan and Vesse [10] Mumford-Shah (MS) functional model the curve parameters were determined from minimization of region based energy given by,

$$E_{cv} = \int_{R^u} (I - \kappa)^2 dA + \int_{R^v} (I - \gamma)^2 dA \tag{1}$$

Evolution of the curve in the stochastic domain ensured segmentation of the image ($I$) into two region $u$ and $v$ with mean intensities $\kappa$ and $\gamma$ obtained from posterior probabilities of the two region prostate and the background. In our model, the MS functional of [10] is adopted for the propagation of a region based levelset [10] in the stochastic space to provide the 3D binary segmentation of the prostate in a manner similar to the approach adopted by [7].

## 3 Results

We have validated the accuracy and robustness of our approach with 50 training datasets and 23 test dataset of MICCAI prostate challenge [11]. We have followed the norms of the MICCAI prostate challenge and have used the training data for training our decision forests. Quantitative results were achieved with the training dataset in two fold cross validation method in which 25 datsets were

**Table 1.** Training and testing specifications

| | Specifications | Values |
|---|---|---|
| Algorithm | Packages used | For reading and writing images: ITK, Programming: Matlab |
| | User interaction | Restricted to selection of the first and the last slice of prostate |
| Machine | CPU | Intel Core i5, 2.8 GHz processor |
| | RAM | 8 GB |
| | CPU count | 4 |
| Time | Training time | 3 hrs for 25 datasets (50% of the training datasets) |
| | Testing time | 100 seconds (per dataset) |
| | User interaction time | 20 seconds (Selection of first and last slice ) |

used for training to evaluate the remaining 25 datsets and this was repeated two times to obtain the results for 50 datasets. Qualitative results given in Fig. 3 were achieved with the training datasets. We have fixed the number of trees to 100, tree depth to 30 and the lower bound of information gain to $10^{-7}$ in decision forest. These parameters were chosen empirically as they provided promising results with training images. Manual interaction was restricted to only selection of the first and the last slice of the prostate and the entire process is automatic. The images are not rigidly registered and intensities are not normalized as decision forest has the ability to handle variabilities and yet produce promising results. No region/volume of interest or seed points were selected for the process. Once trained no parameters were tweaked to produce better results for the test images.

During testing, a probabilistic classification of the pixels is achieved with decision forests for each of the apex, central and the base slices. Finally, a region based levelsets propagation in the stochastic space produces a binary segmentation of the prostate in 3D as discussed in 2. The training and testing specifications are enlisted in Table 1. We have used Dice similarity coefficient (DSC) of the apex, central and the base region to evaluate our method for all the training datasets. During quantitative evaluation half of the training dataset were used for building the random forest and tested on the remaining half of the training dataset. This was done two times for each of the apex, central and the base region to achieve the results. The mean and standard deviations for each of the apex, central and the base region are given in Table 2. Qualitative results of our method for some of the test datasets are presented in Fig. 3. It is to be noted that each dataset is composed in two consecutive rows.

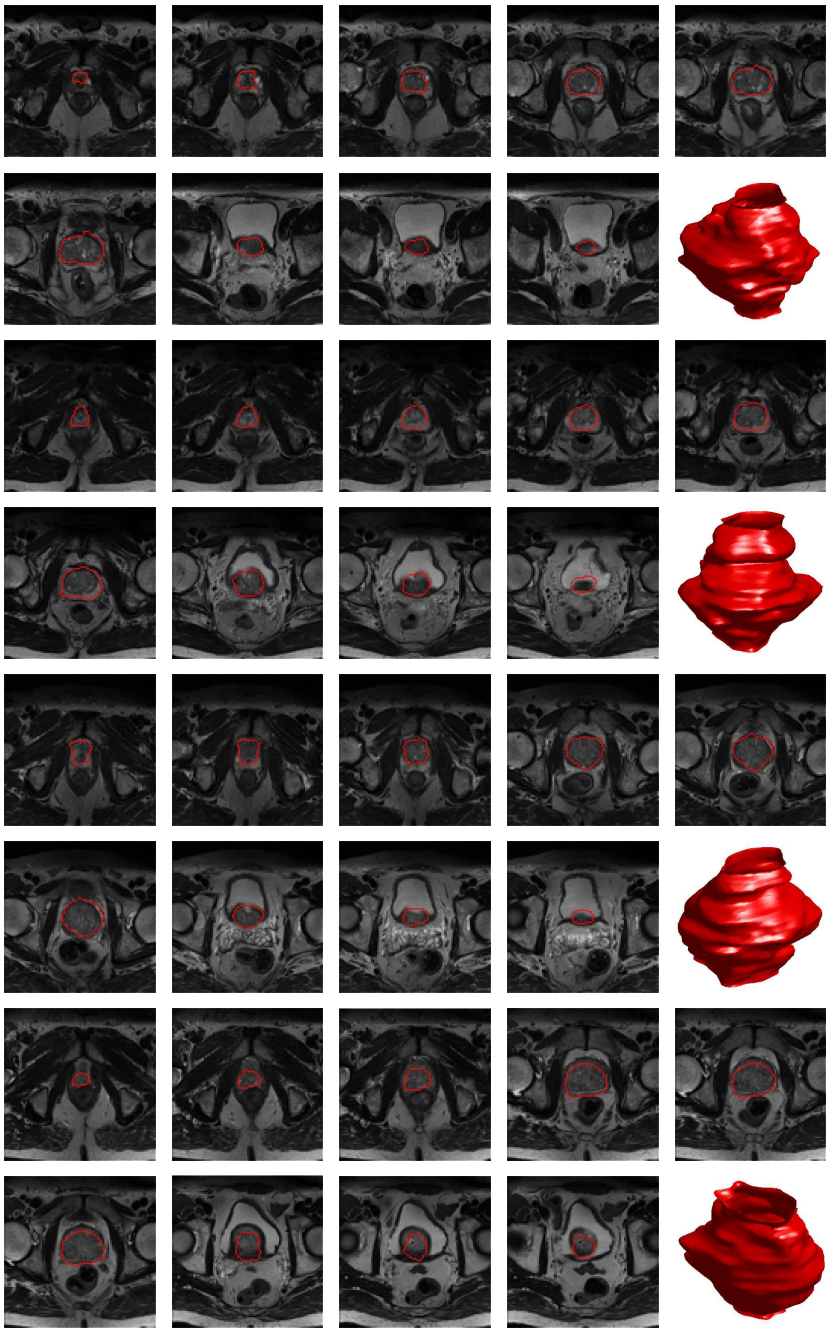

**Fig. 3.** Subset of segmentation results of 4 datasets. The red contour/volume is created from the achieved segmentation.

**Table 2.** Prostate segmentation quantitative results for training datasets

| Region | DSC |
|---|---|
| **Apex** | 0.64±0.18 |
| **Central** | 0.73±0.11 |
| **Base** | 0.61±0.17 |

## 4 Conclusions

A novel schema of probabilistic classification obtained with decision forest with the goal of segmenting the prostate in 3D MRI images has been proposed. Our approach is simple and computationally efficient. The proposed method has shown some promising results however the results could be probably further improved with optimized selection of discriminative features in decision forest and introducing shape and appearance priors in the framework as has been proposed in our previous work in [12].

## References


1. Cancer Society Atlanta, A.: Prostate Cancer. www.cancer.org, accessed on [28th Jan, 2012] (2011)
2. Klein, S., van der Heide, U.A., Lipps, I.M., Vulpen, M.V., Staring, M., Pluim, J.P.W.: Automatic Segmentation of the Prostate in 3D MR Images by Atlas Matching Using Localized Mutual Information. Medical Physics **35** (2008) 1407–1417
3. Martin, S., Troccaz, J., Daanen, V.: Automated Segmentation of the Prostate in 3D MR Images Using a Probabilistic Atlas and a Spatially Constrained Deformable Model. Medical Physics **37** (2010) 1579 – 1590
4. Dowling, J., Fripp, J., Chandra, S., Pluim, J.P.W., Lambert, J., Parker, J., Denham, J., Greer, P.B., Salvado, O.: Fast automatic multi-atlas segmentation of the prostate from 3d mr images. In Madabhushi, A., Dowling, J., Huisman, H.J., Barratt, D.C., eds.: Prostate Cancer Imaging. Volume 6963 of Lecture Notes in Computer Science., Springer (2011) 10–21
5. Gao, Y., Sandhu, R., Fichtinger, G., Tannenbaum, A.R.: A Coupled Global Registration and Segmentation Framework with Application to Magnetic Resonance Prostate Imagery. IEEE Transactions on Medical Imaging **10** (2010) 17–81
6. Toth, R., Tiwari, P., Rosen, M., Reed, G., Kurhanewicz, J., Kalyanpur, A., Pungavkar, S., Madabhushi, A.: A magnetic resonance spectroscopy driven initialization scheme for active shape model based prostate segmentation. Medical Image Analysis **15**(2) (2011) 214–225
7. Li, W., Liao, S., Feng, Q., Chen, W., Shen, D.: Learning image context for segmentation of prostate in ct-guided radiotherapy. In: MICCAI. Volume 6893. (2011) 570–578
8. Geremia, E., Menze, B.H., Clatz, O., Konukoglu, E., Criminisi, A., Ayache, N.: Spatial decision forests for ms lesion segmentation in multi-channel mr images. In: MICCAI. Volume 6361. (2010) 111–118

9. Zuiderveld, K.: Graphics gems iv. Academic Press Professional, Inc., San Diego, CA, USA (1994) 474–485
10. Chan, T.F., Vese, L.A.: Active Contours Without Edges. IEEE Transactions on Image Processing **10** (2001) 266–277
11. MICCAI: 2012 prostate segmentation challenge MICCAI. http://promise12.grand-challenge.org, accessed on [21st May, 2012] (2012)
12. Ghose, S., Oliver, A., Martí, R., Lladó, X., Freixenet, J., Mitra, J., Vilanova, J.C., Comet, J., Meriaudeau, F.: Multiple mean models of statistical shape and probability priors for automatic prostate segmentation. In Madabhushi, A., Dowling, J., Huisman, H.J., Barratt, D.C., eds.: Prostate Cancer Imaging. Volume 6963 of Lecture Notes in Computer Science., Springer (2011) 35–46